

Assessment and analysis of damage in L'Aquila historic city centre after 6th April 2009

Dina F. D'Ayala · Sara Paganoni

Received: 27 April 2010 / Accepted: 24 October 2010 / Published online: 30 November 2010
© Springer Science+Business Media B.V. 2010

Abstract The paper describes the output of a survey carried out in the district of L'Aquila, Italy, in May 2009 after the April earthquake and later in January 2010, and the consequent vulnerability assessment completed by the authors. Observations collected on site regard masonry buildings of the historic centre of L'Aquila and the towns of Paganica and Onna; particular focus was given to a number of buildings of interest, which better represent two locally recurrent building typologies: the mansion and the common dwelling. A description of the main structural features and their influence on damage mechanism is provided, stressing the importance of elements such as wall lay-out, quality of masonry and strengthening interventions. The gathered information is used as input for the application of the FaMIVE method (D'Ayala and Speranza in *Earthq Spectra* 19(3):479–509, 2003), whereby feasible collapse mechanisms and the associate failure load factors can be identified. The procedure is briefly outlined and results are discussed from the point of view of the performance point: push-over curves produced by statistical elaboration of FaMIVE's output are compared both with the demand spectra obtained from EC8 and the response spectrum for the main shock as recorded by the closest station to the town. Conclusions are drawn on the reliability of the FaMIVE method with respect to its capability of predicting the damage mechanism identified on site.

Keywords L'Aquila · Seismic vulnerability · Masonry structures · Historic centres

1 Introduction

The earthquake of 6th April 2009 and its aftershocks have caused extensive damage to a large historic urban area in Italy. Although previous events of the last two decades, Umbria and Marche, 1997; Molise Region, 2002; Garda Lake, 2004, had severely damaged the Italian historic building stock, they have not affected a major historic centre such as L'Aquila, with

D. F. D'Ayala · S. Paganoni (✉)
Department of Architecture and Civil Engineering, University of Bath, Bath BA2 7AY, UK
e-mail: S.Paganoni@bath.ac.uk

a plan area of about 1.5 km² and a resident population within the city walls of at least 10,000 people.

The case of L'Aquila is most emblematic and unique from both conservation and seismic points of view, for a number of reasons: the city includes within its walls a building stock up to 700 years old and varied in age and architectural styles; its heritage buildings are not limited only to monumental or religious buildings, but constitute the urban fabric and residential stock; its history is marked by a number of previous destructive earthquakes and the evidence of historic reconstruction and repairs is clearly visible.

Many of the existing historic buildings have undergone substantial re-adaptation and changes to their structural system in the last 50 years to account for better exploitation of space, insertion of modern residential comforts and limitedly to improve their seismic performance. Therefore an assessment of their seismic vulnerability with relatively simple methods is difficult due to the several uncertainties of behaviour associated with the present construction characteristics.

The presence in literature of procedures for displacement based vulnerability assessment of historic masonry is very modest. Among the methods available, those based on mechanism identification are particularly suitable for use within displacement based performance assessment (Lang and Bachmann 2004; D'Ayala 2005, 2008; Lagomarsino and Giovinazzi 2006; Crowley et al. 2004; Bernardini and Lagomarsino 2008; Restrepo-Vélez 2003). This type of model associates capacity curves to specific construction characteristics or building typologies, which can be considered as having a homogeneous response to seismic hazard. Capacity curves are usually defined assuming either in-plane or out-of-plane failure behaviour and quantifying strength and displacement by computing simple geometric parameters (cross sectional area of walls at chosen levels, inter storey height, etc) and very few mechanical parameters (such as characteristic shear strength or coefficient of friction and compression strength) which can be inferred on the basis of the knowledge of the materials or by limited testing. The definition on the capacity curve of specific limit states (corresponding to predefined displacement values) and correlation of these to damage states eventually allows the distribution of different damage levels over a population of buildings (a mean damage value and standard deviation) to be defined and hence the fragility curves for different levels of shaking to be derived. One of the advantages of such approach is that since it allows for evaluating the capacity of the structure as an analytical function of a modest number of geometrical and mechanical parameters, it is possible to apply suitable procedures for the uncertainty propagation (Pagnini et al. 2008). In recent years procedures to derive fragility curves for building stocks in some European cities have been developed within EU-funded projects such as RISK-EU (Spence and Brun 2006) and LESSLOSS (Spence 2007; Spence et al. 2008). However, these procedures are often based on an empirical approach rather than the analytical approach outlined above.

A robust analytical procedure needs extensive validation by correlating its damage estimates with observed earthquake damage data, and verifying that the chosen parameters are representative of the building stock, both in terms of hypothesis of structural behaviour (flexible versus rigid horizontal structures, out-of-plane versus in-plane resisting mechanism, etc.) and actual numerical values.

The use of a procedure, proposed by D'Ayala (2005), which can be considered as a development of the N2 method for masonry structures (Dolsek and Fajfar 2004), is presented here, to analyse the earthquake effects on the historic centre of L'Aquila. It uses limit state analysis with a mechanism approach to obtain realistic pushover curves for structural masonry components and has been coded within the FaMIVE procedure (D'Ayala and Speranza 2003). Given the non standard nature of existing masonry buildings, the procedure is interfaced with

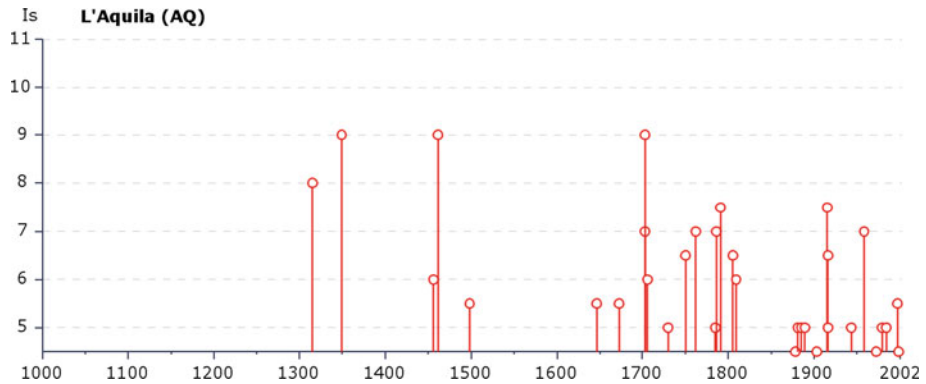


Fig. 1 Historic earthquakes felt in L'Aquila from year 1000 to 2002 (source: INGV Database Macrosismico Italiano-2008, at <http://emidius.mi.ingv.it/DBMI08/>). Is is the Intensity at the site in MCS scale. (Stucchi et al. 2007)

a database from post-earthquake damage and construction surveys, which allows for correlating specific masonry construction details with seismic performance and damage states. The procedure has been validated with empirical data from various seismic events and applied to define risk scenarios in Europe and Asia (Bernardini and Lagomarsino 2008; D' Ayala and Ansal 2009).

The results of two campaigns of survey of the historic centre of L'Aquila are reviewed in the next section, highlighting construction characteristics and corresponding damage patterns. The gathered information is used as input for the application of the FaMIVE procedure, whereby feasible collapse mechanisms and the associate failure load factors can be identified. The procedure is briefly outlined and results are discussed in terms of performance points: push-over curves produced by statistical elaboration of FaMIVE's output are compared both with the response spectra as obtained from EC8 and the response spectrum for the specific main shock, as recorded by the instrument closest to the city centre. Fragility curves are then derived for different limit states, both in terms of lateral capacity and lateral displacements.

2 On-site survey

2.1 Construction characteristics

During two on-site visits to L'Aquila and the villages of Paganica and Onna, the authors carried out a detailed post-event survey of the historic centre of L'Aquila focusing on unreinforced masonry (URM) structures. In particular, attention was paid to residential and ordinary buildings, which form the historic fabric of L'Aquila city centre. These have been erected from the thirteenth century onward, with the largest portion being built after the 1703 earthquake, which, together with the 1349 and 1453 events, had a destruction potential comparable to the 2009 event (Fig. 1).

Within the residential stock two main building typologies can be identified (Fig. 2): common buildings, which nowadays are used as dwellings and small commercial activities, and small to large mansions, which have either residential or administrative functions. Although sometimes substantially different in term of dimensions, the quality of materials



Fig. 2 **a** Apartment building from late nineteenth century and **b** mansion from early 20th century

and construction is fairly homogeneous, with a high concentration of mansions in the historic centre of L'Aquila, where most of the wealthy families of the province used to reside.

Common buildings are from two (older and poorer) to four-storey high (mostly built in the last 200 years), grouped in bulk-shaped blocks, formed by a relatively regular street grid (see map in Fig. 15). Buildings within the blocks were in some cases built all at the same time, as it is visible from the interlocking of the masonry work among common party walls, or in other cases over time, with adjacent buildings having independent party walls and different floor height, even though no space might have been left between the facades. In a small number of cases, reinforced concrete frame buildings are also present in adjacency to masonry houses. This layout has direct implications on the seismic behaviour of single buildings and clusters, and leaves some of them at severe risk of hammering, as indeed was observed. A block is formed by four to eight buildings, usually arranged around small internal courtyards, each with dimensions variable in function of the number of rooms, these normally being a standard size of $3\text{--}4 \times 4\text{--}5$ m. Mansions tend to be larger and isolated, covering a whole block, or arranged in less numerous clusters, showing regular plan layout. While no high-rise structures exist in the city centre, buildings within a block might present variable height, with differences up to two storeys.

The bearing system is composed by sets of orthogonal walls, the original alignment being frequently compromised as a result of modifications brought to structures throughout the years. Typical alterations to the original structure are the frequent addition of a storey above the original roof level, and the inclusion of mezzanines in those cases where original storey height was more than 4.5 m. The effect of this continuous remodelling of internal spaces, sometimes leading to fusion of two or more buildings into new ones, can also be observed in the masonry fabric: walls, which are from half to a meter thick, feature different quality and typology of units and mortar, in some cases mixed together in the very same wall, sometimes with additions of concrete blocks, steel beams and r.c. slabs replacing original floors (Fig. 3).

Masonry fabric typologies most frequently observed were rubble stone, roughly squared stone blocks mixed with bricks, sometimes in regular courses, brick masonry, and dressed stone blocks. Walls in a few cases appear to be massive, but most commonly are formed by the so called “*muratura a sacco*”, namely two wythes of dressed stones poorly connected, sometimes with a rubble infill. (Fig. 5a) Mortar is mainly lime mortar, but mud mortar was observed in the village of Onna (Fig. 4). Large squared stone blocks are used for quoins both in common buildings and mansions (Fig. 5b, c) but the overall quality of material and workmanship is generally superior in the latter thanks to the use of courses of dressed stone



Fig. 3 Example of masonry fabrics with later addition of upper storey and concrete elements

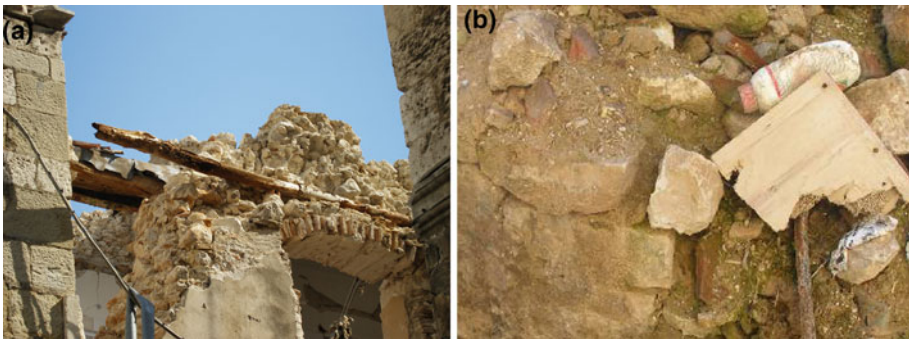


Fig. 4 Typologies of mortar surveyed on site: **a** lime mortar in L'Aquila and **b** mud mortar in Onna


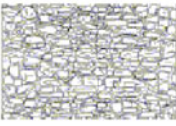



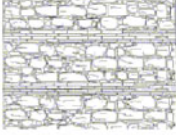

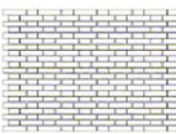


Fig. 5 Examples of **a** 'muratura a sacco' and of **b–c** stone quoins. The photo on the right is of a building of the XIV century in which two storeys have been added under and above the original roof line

alternating to courses of brickwork. It should be noted that, although an accurate case by case study could not be conducted in this occasion, generally the quality of the masonry fabric is related to the age of the building, with buildings predating the 1703 earthquake showing better choice of stone units, regularly dressed and laid out in thin bed joints of good lime mortar.

Table 1 shows images of the typologies of masonry identified on site, classifies them according to the FaMIVE procedure, and correlates them to the classifications proposed by the Italian Gruppo Nazionale per la Difesa dai Terremoti, CNR-GNDT (Bernardini 2000) and by the Italian code Ordinanza (OPCM) 3274 (Consiglio dei Ministri 2003). The CNR-GNDT

Table 1 Mechanical properties of the surveyed typologies of masonry as referred by Italian seismic guidelines and codes. f_m indicates the range of compressive strength, t_m indicates the range of characteristic shear strength

On-site survey and FaMIVE classification	CNR-GNDT	Annex 2-OPCM3274	
		f_m (N/mm ²) min-max	t_m (N/mm ²) min-max
 <p>C1: Rubble stone</p>	 <p>Rubble random stone masonry</p>	6.0-9.0	0.2-0.32
 <p>D2: Cut stones with randomly inserted bricks</p>	 <p>Roughly shaped stone blocks, random bricks</p>	11.0-15.5	0.35-0.51
 <p>D1: Squared stones with regular brick courses</p>	 <p>Roughly shaped stone blocks, with binding brick courses</p>	15.0-20.0	0.56-0.74
 <p>B1: Brickwork</p>	 <p>Brickwork</p>	18.0-28.0	0.6-0.92

classification includes a table of typical masonry layouts to be used during post-earthquake surveys: each masonry type is subdivided in two categories depending on the type of fabric and mortar, and the presence of binding brick courses and internal connections. The quality of the fabric is directly correlated to the capacity to resist in-plane and out-of-plane collapse mechanisms.

The masonry types identified by the CNR-GNDT classification can be related, through their description, to typical ranges of compressive and shear strength suggested by Annex 2 of OPCM 3274, providing an initial characterisation of materials. It is worth noting that the ranges are in some cases rather wide and overlapping, implying substantial difference in performance.

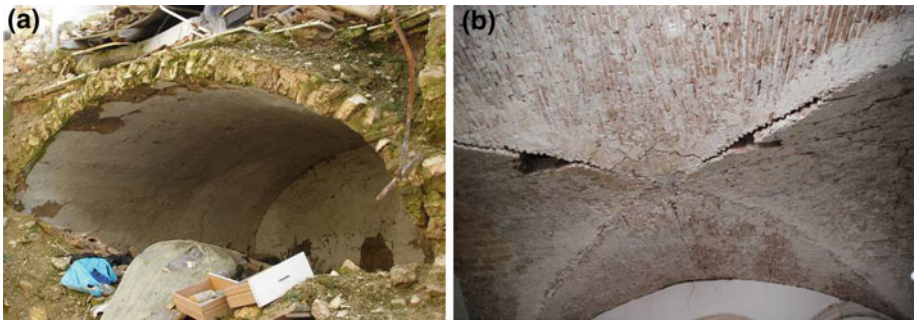


Fig. 6 Typologies of vault: **a** barrel vault built with roughly shaped stone with a thickness of about 0.25 m, and **b** shallow brickwork cross vault, with bricks laid in folio and overall thickness of 0.06 m

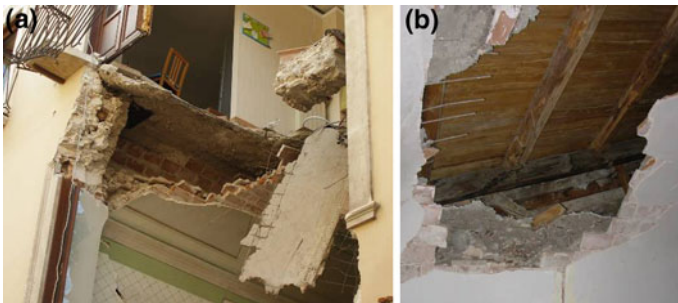


Fig. 7 **a, b** Brickwork in folio vaults introduced after the 1703 earthquake as false ceilings, altered into load bearing elements by the introduction of a wire net reinforced concrete screed in the late twentieth century

The original horizontal structures surveyed in L'Aquila include both masonry vaults and timber floors and roofs, replaced in recently refitted buildings by lightweight jack arches on steel beams. Masonry groin and low-rise vaults are generally present at the ground floor (Fig. 6), especially in mansions, over the main entrance and to support staircases. Decorative groin vaults were introduced as false ceilings after the 1703 earthquake and are common also at upper levels. Although these were not originally structural elements, they have indeed been used for this purpose, by laying concrete screed floors with steel mesh on top of them (Fig. 7). As in many other historic centres in seismic prone areas, cross-ties are a common feature, introduced certainly since the 1703 earthquake, but in some case probably even before. Traditionally made of timber with a iron end plate, more recently and commonly, wholly of iron (Fig. 8), they are inserted longitudinally into the masonry, just below the floor level or above the openings, with metallic plates or elements resting on the external surface of the wall to improve the connection between sets of perpendicular walls or between walls and floor joists. Many modern typologies made of stainless steel are also visible. The ties and quoins have the aim of improving the box-like behaviour of the masonry cell. A qualitative assessment of their performance is presented in the following section by way of analysis of the observed damage.

2.2 Description of damage

The damage observed in L'Aquila has been classified using the catalogue of mechanisms originally developed for the FaMIVE procedure by [D' Ayala and Speranza \(2002\)](#), with later



Fig. 8 Traditional reinforcement: **a** timber tie, **b** wrought iron cross tie inserted in a quoin and **c** twentieth century steel tie with end plate

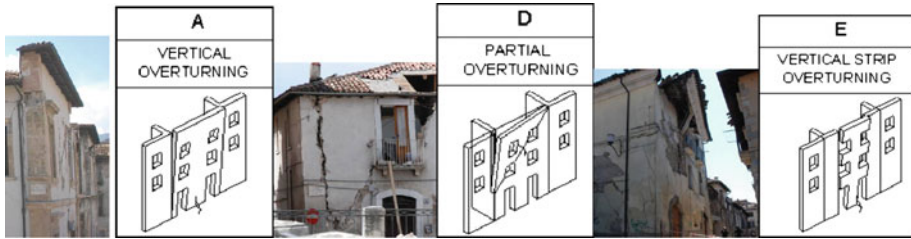


Fig. 9 Out-of-plane mechanisms due to poor connections at corners: damage mechanism A, complete overturning of façade; damage mechanism D, partial overturning along a diagonal, mechanism E, partial overturning of the openings vertical strips

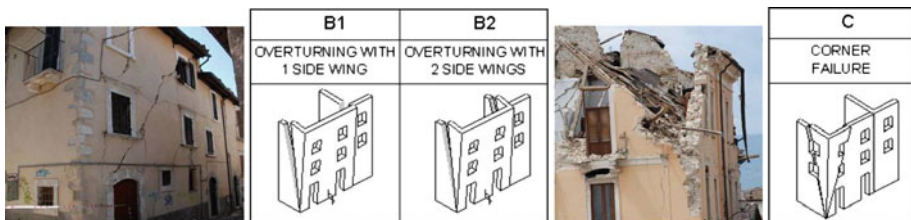


Fig. 10 Effect of good connections at corners: damage mechanism B, overturning with side wing/s (*left*), and damage mechanism C, corner failure (*right*)

additions and updates. While the actual proportion of each damage type, within the surveyed sample will be presented in Section 3 and compared with the calculated damage mechanisms, here a qualitative correlation between construction details and damage types from visual inspection of a larger number of buildings is established. Both parameters relate to the observed behaviour of the visible façades, as most of the buildings were inspected from the street only, given safety and security concerns. The partial or total overturning of the façade is due to poor quality of connections between walls or part of them, as shown by photos and sketches in Fig. 9. When the quality of the masonry fabric at the corner is enhanced by the presence of quoins, the façade is not allowed to overturn and mechanism types B or C will preferably develop (Fig. 10). The occurrence of one or the other of the two types depends on the layout of the opening, on the spanning direction of the horizontal structures and on the presence of internal load bearing walls normal to the façade and their connection to it. However, the efficacy of cut stone quoins is limited when coupled with poor fabric or internally unconnected masonry as walls don't behave like rigid bodies but tend to become loose. It should also be noted that in some cases the quoins might be only veneers inserted for architectural rather than structural purposes.

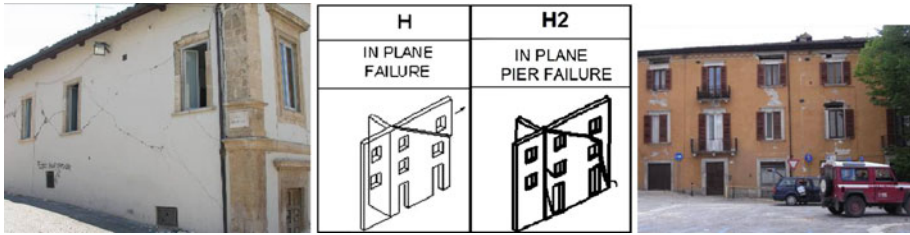


Fig. 11 In-plane damage mechanism in pier, H (left), and combined in piers and spandrels, H2 (right)

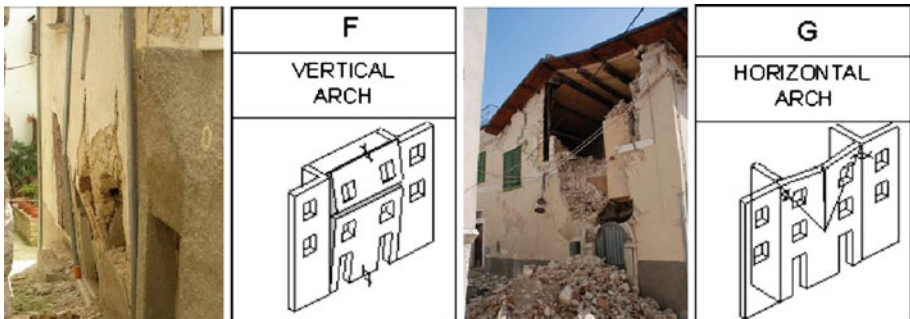


Fig. 12 Damage mechanism F—vertical arch (left) and damage mechanism G—horizontal arch (right)

When out-of-plane mechanisms of the types described above are prevented by efficient connections among orthogonal walls then in-plane mechanisms, mainly activating the shear capacity of the masonry, are likely to develop. Differently from what usually considered in modern unreinforced masonry, the occurrence of regular diagonal X shaped cracks in the spandrels or in the piers is not the most common case. This is due to various issues: firstly, the irregular distribution and size of opening leads to uneven distribution of stiffness and shear capacity among the piers so that some might be more vulnerable than others; secondly, even when the opening layout is orderly and regular, if the floor structures are not rigid in their plane, as it is the case with timber floors and vaults, the redistribution among piers of the lateral actions will depend on their connections with internal walls and position of the timber beams or groin of the vault.

Furthermore the piers might be failing in a combination of bending and shear, rather than just shear (Casapulla and D’Ayala 2006). For these reasons mechanisms H and H2 depicted in Fig. 11 are calculated by identifying the weakest load path in the façade leading to shear failure, rather than simply using lateral capacity of the piers and assuming a rigid behaviour of the spandrel. Cross-ties, which originally might have been introduced to counteract the thrust generated by vaults, also help to protect the façades from out-of-plane damage in a large number of cases. When the façade is prevented from moving out at the roof level and along the edges, it might behave like a constrained plate, with out-of-plane movement at a lower level. When the mechanism fully develops is identifiable by the bowing out of the walls (Fig. 12). However for the constraints to be effective the ties should be regularly spaced over the façade and correctly anchored and connected through to the orthogonal walls or to the floor structure. When this is not the case, and the unrestrained length of the façade is considerable in respect to its thickness, then mechanism type G is likely to occur.

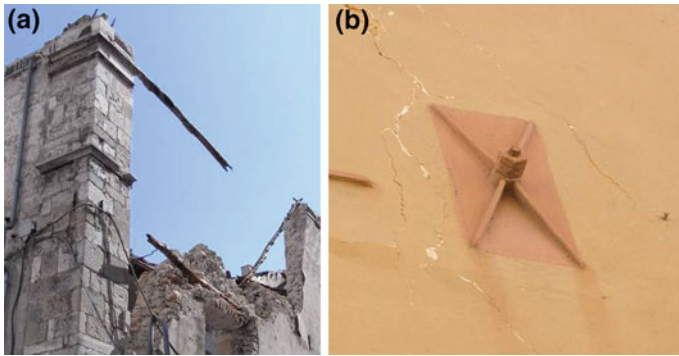


Fig. 13 Examples of failed steel cross-ties: **a** material failure by tension of a timber tie; **b** punching shear failure of the anchor plate through the masonry wall



Fig. 14 Collapse of roof structures

Examples of poor performance of ties were observed, related to either material deterioration of the anchor (Fig. 13a), mainly in the case of timber, or lack of sufficient integrity and shear capacity in the masonry to withstand the thrust generated at the anchoring plate by the relative movement of the two orthogonal walls (Fig. 13b).

The quality of masonry dramatically influenced the level of damage: the difference is between local or total collapse in the ordinary houses made of rubble or poorly squared stonework, and damage limited mainly to cornices, lintels and other jutting elements, or slight separation of perpendicular walls at the level of the spandrels, in the cases of better built mansions. In many of the latter group the internal partitions suffered important shear diagonal cracks and in a limited number of cases also separation from the orthogonal façade walls, but in general collapse was prevented.

The quality of masonry was also a contributing factor for other associated failures observed: indeed the partial or total collapse of floors and roofs recurred frequently, due to the high deformations occurring in the walls, enhanced by the thrusting action of the horizontal structures themselves, which caused the bearings to slip out of their positions (Fig. 14).

In summary, within the historic city centre of L'Aquila the number of total collapses observed was minor, while the proportions of partial collapses of the upper storeys was perhaps greater than would have been expected given the level of shaking. In a minority of cases total collapse of the façade was observed, and these were usually associated to substantial alteration of the original structure. Although the number of masonry buildings undamaged is very modest, the majority suffered either minor damage or structural repairable

damage. This situation allows on one hand to identify and recognise collapse mechanisms, on the other to better correlate ultimate capacity to strong motion characteristics, and hence lends itself to a more detailed in situ survey and analytical assessment, as discussed in the following section.

3 Vulnerability assessment procedure and collapse mechanism identification

3.1 Definition of sample and data collection

During two campaigns of survey, in the first week of May 2009 and in January 2010, a sample of ninety buildings was surveyed, recording geometric layout, construction and structural details for at least two orthogonal elevations and floors and roof structures. The location of the buildings was chosen to reflect the different typologies present and the different levels of observed damage across the city centre. A minority of buildings (10%) was assessed only from photographs.

The form used for the survey is shown in Fig. 25 (Appendix). Given the open-ended approach of the FaMIVE procedure, the form is updated routinely when applied to a new site in order to tailor the survey to the specific identified construction typologies, enriching the FaMIVE database with new structural details, connections systems and masonry fabrics (see for instance application to Nepalese and Indian building samples, in [D'Ayala and Yeomans 2004](#); [D'Ayala and Kansal 2004](#), respectively). These details are then interpreted in terms of structural behaviour and their influence on the development of specific failure mechanism is accounted for in the algorithms. For instance, given the substantial presence of vaulted structures at ground or first floor level in many buildings in L'Aquila and their evident influence on the overall seismic response, their geometry, type and setting is recorded in detail and their effect on the load bearing walls accounted for, both in terms of mass and lateral trust. The type of damage mechanism and level of damage observed are also recorded for each elevation surveyed. Six damage levels from 0 to 5 are considered, broadly corresponding to the EMS'98 definitions for masonry structures ([Grunthal 1998](#)). Because in the survey the damage levels are recorded as associated to the mechanism believed to have caused the damage (section 7 of the form) and, as more than one mechanism might have developed to different extent, different levels of damage can be recorded for the same façade elevation.

The database of parameters collected during the survey allows the provision of a first statistical picture of the building stock in L'Aquila and of its damage state. The results can be compared with the results obtained by the surveys carried out by the Protezione Civile in collaboration with the Ministry of Cultural Heritage for selected mansions (Modello B-DP PCM-DPC, Protezione Civile 2006), or with the AeDes survey for ordinary buildings ([Baggio et al. 2000](#)), to obtain a more complete picture. Some of these results are discussed in other papers within this special issue ([Tertulliani et al. 2010](#), [Binda et al. 2010](#)).

The location of surveyed buildings is recorded on the map of Fig. 15, together with the maximum level of damage and prevalent failure mechanism observed for each façade. Samples have been chosen to form small clusters in each of the Quattro Cantoni of the town, typically around a square or religious building, and to cover buildings of different ages. An almost equal proportion of buildings shows a maximum level of damage 2 (28%), 3 (32%) or 4 (26%), with a minority showing damage 0–1 (5 %) or 5 (6%).

The sample has been divided into five categories classified by both masonry and floor structure type, according to the catalogue developed for the PAGER project ([D'Ayala et al. 2010](#)): brickwork (corresponding to B1 in Table 1) with flexible horizontal structures (UFB3) or with stiffer horizontal structures (UFB5), dressed stone (D1 in Table 1) with flexible (DS2)

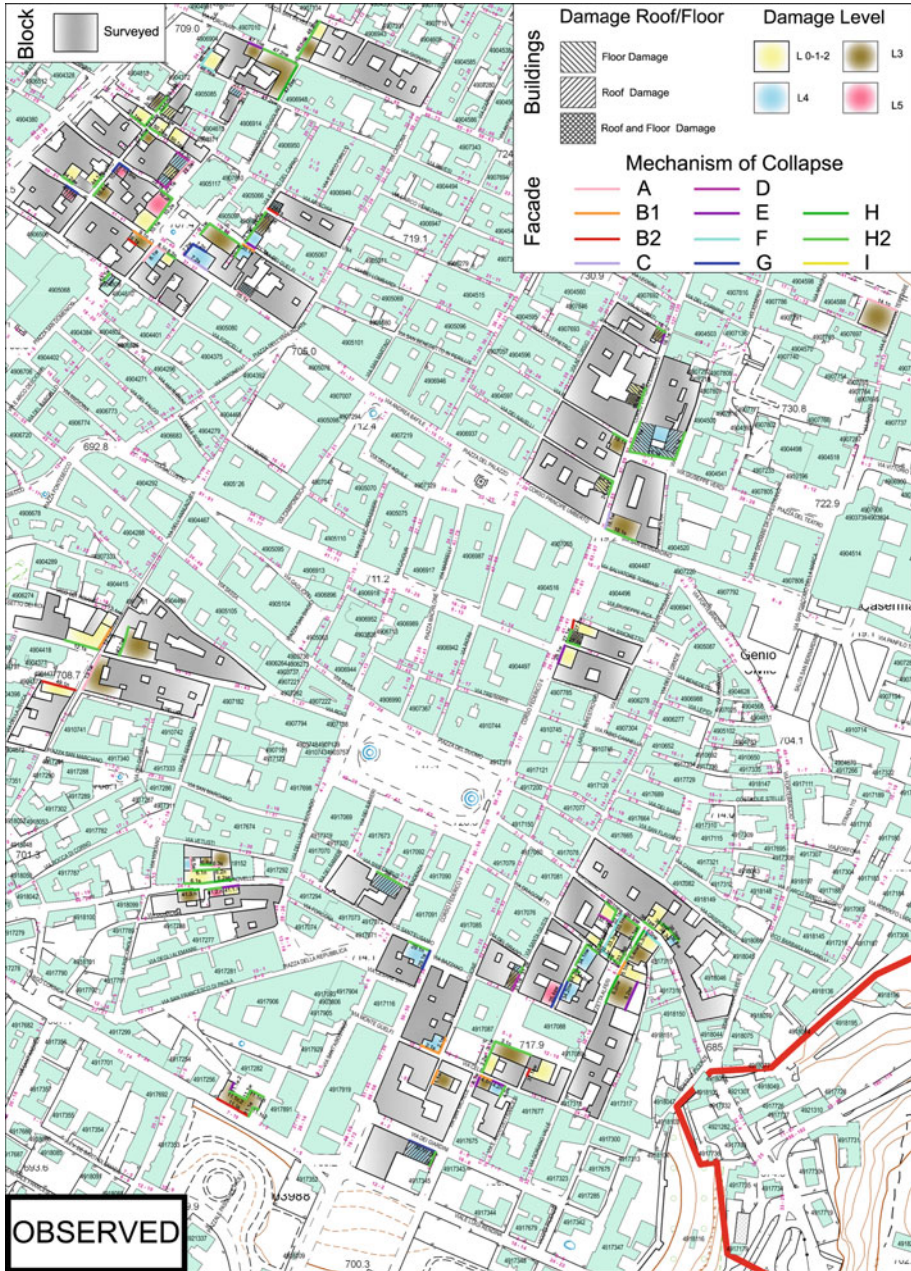


Fig. 15 Localization of the surveyed sample within the historic city centre of L’Aquila. Mapping of observed damage levels and collapse mechanisms of the façades

or stiffer (DS4) horizontal structures, and poorly dressed (D2 in Table 1) and rubble (C1 in Table 1) stonework (RS3). The FaMIVE procedure used to calculate the lateral capacity of the façades does not use the same strength parameters listed in Table 1, but a Coulomb-like criterion (D’Ayala et al. 1997) together with the geometry of the interlocking masonry units.

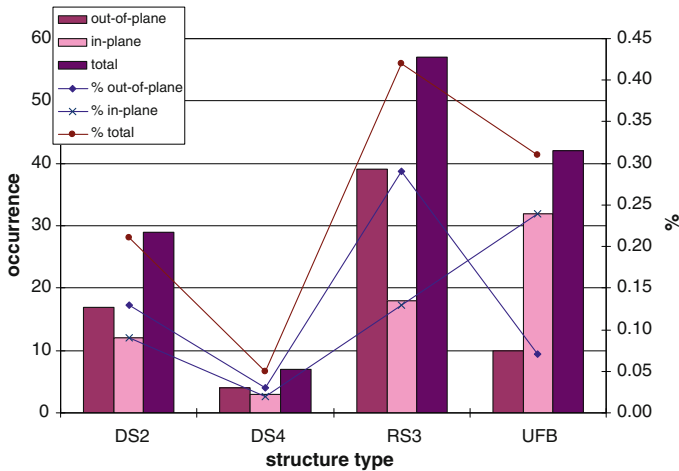


Fig. 16 Distribution of structures types (RS3, DS2, DS4, UFB) and associated in-plane and out-of plane failure mode by façades, within the sample of 90 buildings surveyed with the FaMIVE procedure. For each building typically one or two façades are analysed, depending on access

The FaMIVE procedure calculates the most likely mechanism to occur for a given façade or elevation, with given connections to the rest of the structure, using a limit state analysis and lower bound approach. The procedure calculates first the collapse load factor associated to all possible mechanisms for a wall, i.e. the mechanisms that can develop given the constraint conditions surveyed (as given in Figs. 9, 10, 11, 12), then chooses the “worst” in terms of the highest result of the product between the inverse of the collapse load factor and the damage extent. However often two or more out-of-plane mechanisms might have similar collapse load factors and extent, or the in-plane and out-of-plane vulnerability for a given wall might be of the same level. In this case FaMIVE chooses the mechanism that has the most damaging consequences. Ultimately, the collapse load factor and the damage extent are computed to produce a score for each building which measure the vulnerability of the single buildings. Depending on this score the buildings are divided in 4 normalised classes, low, medium, high and extreme vulnerability. (D’Ayala 2005)

The chart in Fig. 16 shows the number of façades elevations in each structure type, subdivided into in-plane or out-of-plane failure, on the basis of the analysis’ results. The majority of buildings are either made of poorly dressed stone (RS3, 42% of the sample) or dressed stone with either timber floors (DS2, 21%) or steel joist and tiles (DS4, 5%). A third of the building stock surveyed, of more recent construction, is made of brickwork with timber floors or concrete slabs (UFB, 31%). According to the assessment, the majority of the stone masonry buildings fail in an out-of-plane mechanism, while the brickwork buildings have a majority of in-plane failures. As stated in the general description of damage in Sect. 2, the occurrence of out-of-plane failure is hindered or prevented by presence of quoins or ties, if these are well distributed.

3.2 Definition of capacity curves and identification of performance points

Besides calculating the ultimate lateral capacity associated with the most vulnerable mechanism, in order to assess and predict levels of damage given a specific strong motion, it is essential to define capacity curves. Capacity curves for masonry have been proposed by various

authors (Tomažević et al. 2004; Lagomarsino and Giovinazzi 2006; Magenes 2006) based on either experimental or empirical evidence. In the present study, on the basis of the observations on site, average capacity curves are developed for each of the building classes identified above. The theoretical background to this approach is presented in D'Ayala (2005). The procedure adopted is summarised in the following. The first step is to calculate the lateral effective stiffness for each wall and its tributary mass. The effective stiffness for a wall is calculated on the basis of the type of mechanism attained, the geometry of the wall and layout of opening, the constraints to other walls and floors and the portion of other walls involved in the mechanism:

$$K_{\text{eff}} = k_1 \frac{E_t I_{\text{eff}}}{H_{\text{eff}}^3} + k_2 \frac{E_t A_{\text{eff}}}{H_{\text{eff}}} \quad (1)$$

where H_{eff} is the height of the portion involved in the mechanism, E_t is the estimated modulus of the masonry as it can be obtained from experimental literature, I_{eff} and A_{eff} are the second moment of area and the cross sectional area, calculated taking into account extent and position of openings and variation of thickness over height, k_1 and k_2 are constants which assume different values depending on edge constraints and whether shear and flexural stiffness are relevant for the specific mechanism.

The tributary mass is calculated following the same approach and it is equal to the volume of the extent of the wall times the masonry density plus the mass of the horizontal structures involved in the mechanism. Effective mass and effective stiffness are used to calculate a natural period, for an equivalent single degree of freedom oscillator. The mass is applied at the height of the centre of gravity of the collapsing portion, with respect to the ground and a constant acceleration distribution over the wall height is assumed. For out-of-plane mechanisms the acceleration and displacement values defining the elastic limit, can be computed as follows. The elastic limit acceleration A_y is identified as the combination of lateral and gravitational load that will cause a triangular distribution of compression stresses at the base of the overturning portion, just before the onset of partialisation. This can be calculated as:

$$A_y = \frac{t_b}{6h_o} g \text{ with corresponding displacement } \Delta_y = \frac{A_y}{4\pi^2} T^2 \quad (2)$$

where t_b is the effective thickness of the wall at the base of the overturning portion, h_o is the height of the overturning portion, and T the natural period of the equivalent SDF oscillator. For in-plane mechanisms a similar equation is applied assuming a compressive strut in each pier with t_b and h_o equal to the width of the strut and the inter storey height respectively. The next point on the pushover curve corresponds to the conditions of maximum lateral capacity A_u :

$$A_u = \frac{\lambda_c}{\alpha_1} \quad (3)$$

where λ_c is the load factor of the collapse mechanism chosen, calculated by FaMIVE, and α_1 is the proportion of total mass participating in the mechanism. This is calculated as the ratio of the total mass of the façade and sides or internal walls and floor involved in the mechanism. The corresponding displacement at incipient collapse is identified by the condition of loss of vertical equilibrium which, for overturning mechanisms, can be computed as a lateral displacement of the top of the wall

$$D_u = t_b/3 \quad (4)$$

with t_b wall thickness at the base of the overturning portion.

An intermediate point between (D_y, A_y) and (D_u, A_u) can also be identified, which corresponds to the position of the resultant of stresses for the fully partialised cross section at

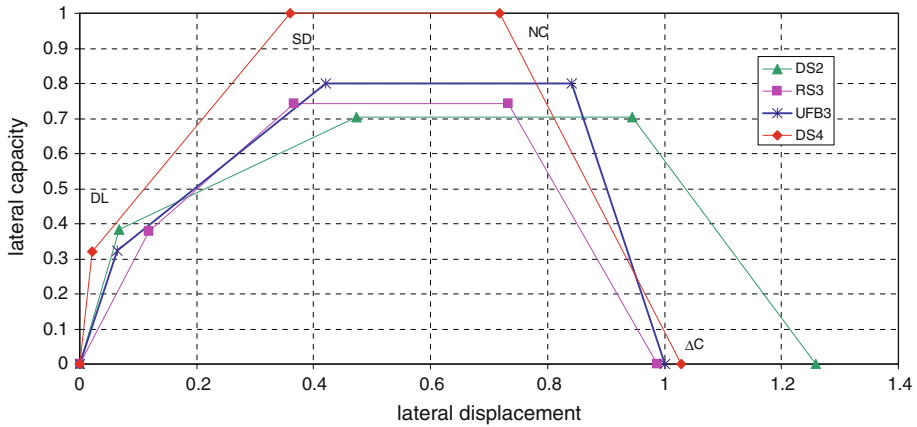


Fig. 17 Normalised and linearised average capacity curves for each of the structure types in L'Aquila city centre

the base. If a parabolic stress block is assumed, the corresponding relative displacement of the top to the base is $D_{sd} \approx t_b/6$. This results in a value of ductility $m = D_u/D_{sd} = 2$, and is conceptually equivalent to defining a q factor.

The 3 points identified can be associated to corresponding state of damage as proposed in Fig. 17 where the linearised and normalised curves for each structure type groups are presented. For each curve, DL, *damage limitation*, corresponds to the elastic lateral capacity (D_y, A_y), SD, *significant damage*, corresponds to the peak capacity (D_{sd}, A_u) and NC, *near collapse*, corresponds to incipient or partial collapse (D_u, A_u).

In Fig. 17 a point D_c is also identified corresponding to the displacement causing total collapse, assumed to be either $t_b/2$ or $l/2$, where l is the average length of the masonry units (bricks or stones), depending on which of the two dimensions is critical for the specific collapse mode identified. The average capacity curves for each structure type, shown in Fig. 17, are normalised with respect to the DS4 curve. The line between NC and DC is shown as dashed, as the actual path between these two points cannot be traced with the current modelling. It is noticeable that the DS4 group shows the higher stiffness and capacity, while DS2 has highest ductility, but lowest peak capacity. The rubble stone group is characterised by an almost linear behaviour up to maximum capacity and a very modest post peak ductile range.

In Fig. 18 the average capacity curves are compared with the EC8 (ENV 2005, Eurocode 8) displacement response spectra (ADRS) having assumed a soil type B and the ADRS obtained from the strong ground motion record closer to the city, AQK (download of the corrected time histories from <http://itaca.mi.ingv.it/ItacaNet/>, last accessed 20/04/2010). For both cases, besides the linear spectra also the non linear spectra obtained for a ductility $\mu = 2$ are shown in Fig. 18, this being the level of ductility calculated from the capacity curves. It should be noted that when compared with the non linear EC8 spectrum the performance point for UFB3, DS2 and DS4 falls in the range between SD and NC, while for RS3 the curve falls short of it (Figs. 18, 20).

With respect to the nonlinear spectrum obtained from the record AQK longitudinal component, the situation is slightly more complex, but indicates that, apart from the DS4 type, the other three structure types would all have experienced substantial structural damage. It is worth noting however that the curves shown are affected by the uncertainty associated with the modelling, plus the uncertainty associated with the data collection. This is evaluated

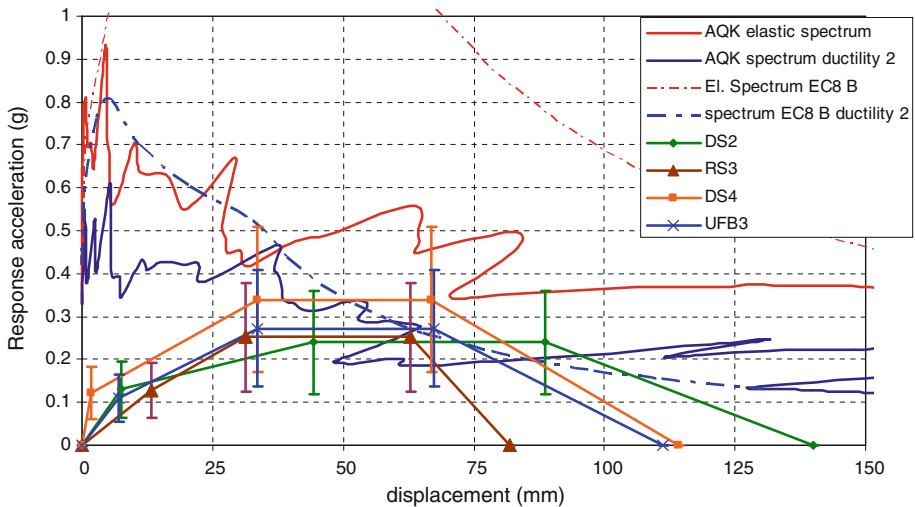


Fig. 18 Comparison of capacity curves for each structure type, including uncertainty range, with the EC8 linear response spectrum for soil type B; the nonlinear response spectra obtained from this by using a ductility $\mu = 2$; the response displacement elastic spectrum for record AQK longitudinal component; the corresponding non linear spectra obtained for the same value of ductility. The non linear spectra have been derived using Seismosoft ©

in terms of reliability of the data for each subsection of the form and is classified as *high*, *medium* and *low*, depending on whether specific data could be measured on site or on drawings, inspected on site, or attributed by photo documentation respectively. In Fig. 18, for each structure type capacity curve, the range of minimum and maximum values of accelerations is also marked for each damage point. The ranges show that only the best performing of buildings DS4 would be able to survive the earthquake within the threshold of structural damage, while the other structural types even at their best performance would have to rely on ductility and hence extensive cracking to survive the earthquake. This shows good correlation with the proportion of maximum observed damage levels reported in Sect. 3.1.

3.3 Correlation between observed and computed mechanisms and level of damage

In order to assess how realistic the capacity curves and performance points obtained for the L'Aquila samples are, a comparison is drawn between observed and computed mechanisms and between relative position of NC collapse point and performance target, and observed damage.

The second consideration relates to the fact that FaMIVE is set to establish the maximum vulnerability as the highest product of the inverse of the collapse load factor times the proportion of building fabric lost for a given mechanism. However in reality a mechanism with a lower load factor and smaller extension of collapse might take place in preference to the FaMIVE lower bound choice. This is highlighted by looking at the correlation between observed and computed mechanisms, mapped in Figs. 15 and 19, respectively.

To carry out this correlation the following assumptions have been made and summarized in Table 2. During the on site survey up to three mechanisms might be associated to a given crack pattern or might be coexisting on the same wall, typically a prevalent, a secondary or possible, and/or a local mechanism (for instance overturning of the upper spandrel and in-plane failure, etc.). For the FaMIVE procedure output, up to two possibilities are considered, corresponding

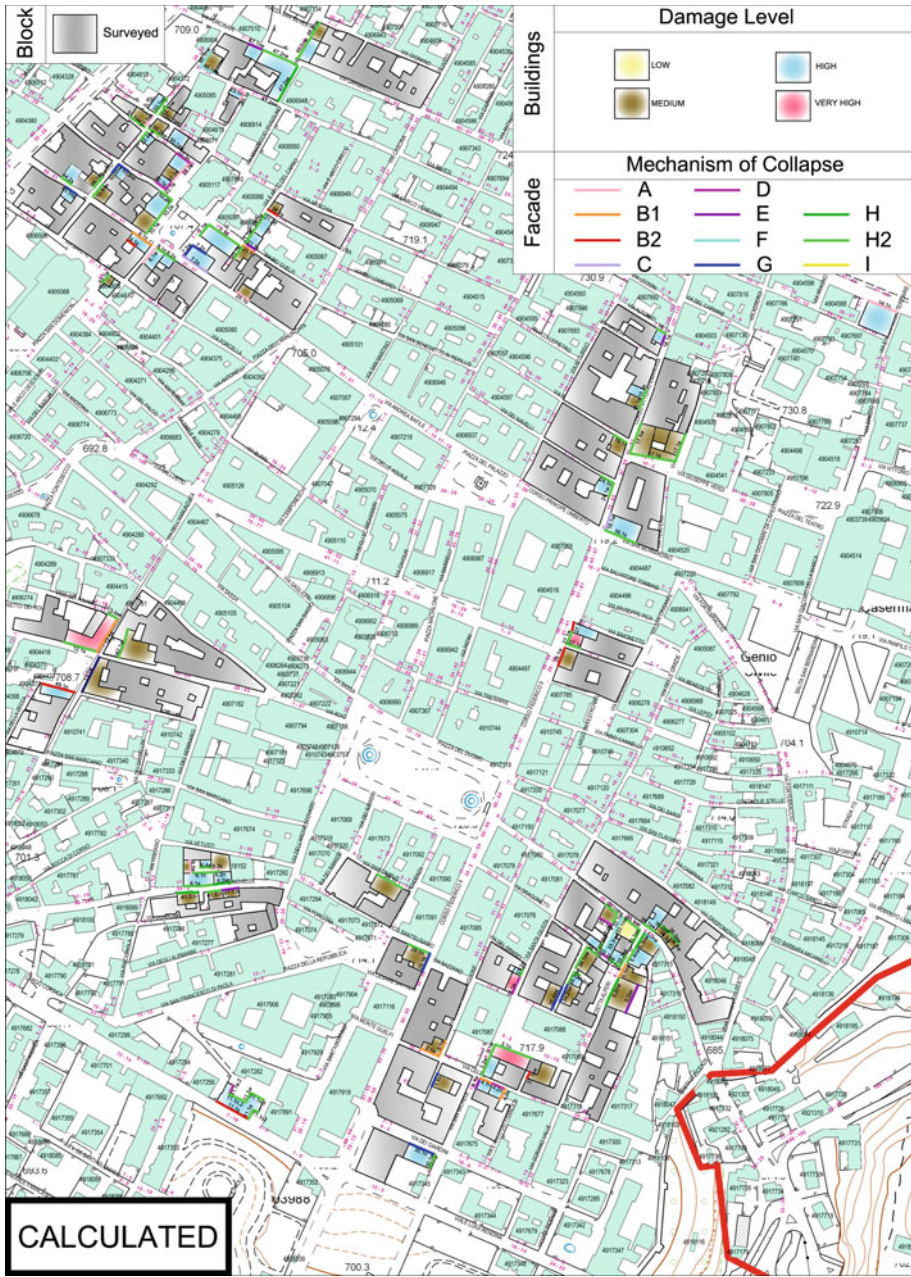


Fig. 19 Mapping of calculated vulnerability levels and mechanisms of collapse for the sample of 90 buildings

to the instance that two mechanisms have very similar collapse load factors and pertain to the same vulnerability class. With these assumptions, a score of 1 is given to the correlation if the first FaMIVE choice matches the prevalent mechanism observed, a score of 2 if it matches the secondary mechanism, and a score of 3 if it matches the local mechanism. If the FaMIVE

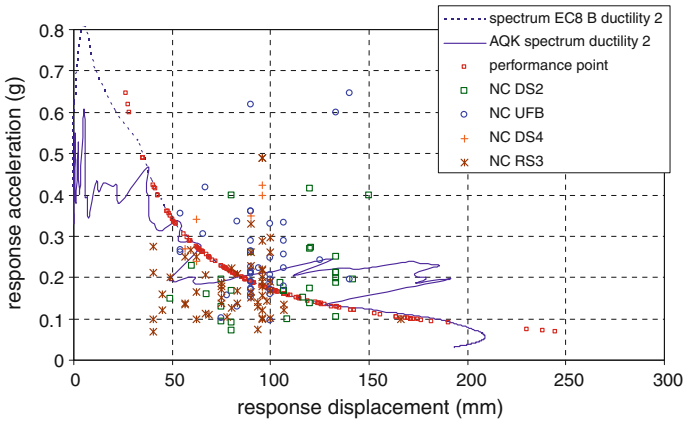


Fig. 20 Correlation between near collapse (NC) point and performance point for the EC8 B response spectrum ($\mu = 2$) for each building by structure type

Table 2 Identification scoring criterion and occurrence

Observed mechanism	Criterion	Predicted Mechanism	Identification Score	Occurrence (%)
Prevalent mechanism	≡	FaMIVE first choice	1	50
Possible mechanism	≡	FaMIVE first choice	2	12
Local mechanism	≡	FaMIVE first choice	3	2
Any of the above	≡	Alternative second choice	4	27
Any of the above	≠	Any of the above	-1	9

■ no correlation

■ prevalent mechanism

■ possible mechanism

■ local mechanism

■ FaMIVE second choice

Fig. 21 Correlation between observed and computed mechanisms

second choice matches any of the observed mechanisms a score of 4 is given. Finally if there is no matching a score of -1 is given.

Table 2 and Fig. 21 show that the prevalent mechanism is correctly predicted in 50% of cases and the alternative worse in 27% of case, while possible and local mechanisms represent a minority, and no correct prediction represent 9% of cases. The results show that there is high correspondence between the basic out-of-plane mechanism and the damage level and the capacity of the programme to predict it correctly. For the in-plane mechanisms H and H2, which account for almost 50% of the sample, the correlation is good.

The calculated mechanisms and vulnerability levels are shown on the map of the historic centre of l’Aquila, in Fig. 19. The sample is evenly shared between medium level vulnerability (45%) and high level vulnerability (48%). A small minority have extreme vulnerability (4.5%) and low vulnerability (2.5%). These values correspond well in statistical terms with the observed level of damage shown in Fig. 15, although with a slight shift towards a more vulnerable scenario than actually observed, as highlighted in Table 3.

As far as the damage is concerned the comparison is carried out by looking at the level of damage observed against the predicted position of the performance point with respect to the

Table 3 Error in estimating the correct damage state for structure typology

Structure type	Underestimate 1 damage state	Correct	Overestimate 1 damage state	Overestimate 2 damage state	Overestimate 3 damage state
DS2	0.10	0.21	0.24	0.28	0.17
DS4	0.14	0.43	0.14	0.28	0
RS3	0	0.25	0.35	0.30	0.10
UFB	0.05	0.27	0.32	0.32	0.04
Total	0.05	0.25	0.3	0.29	0.1

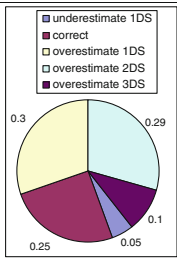
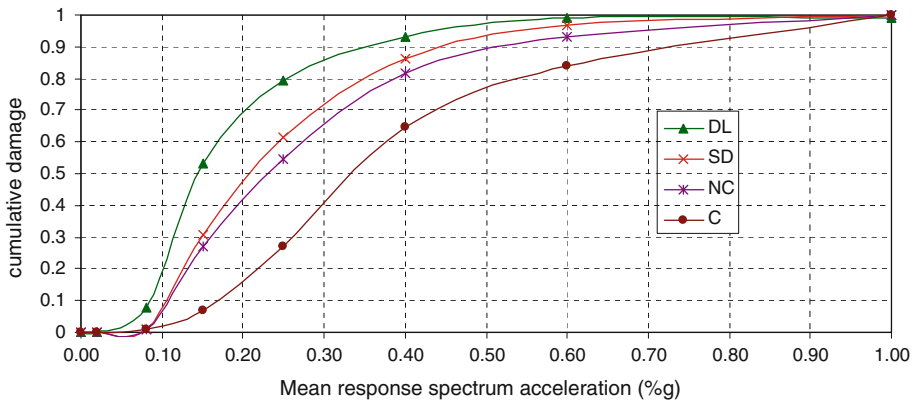



Fig. 21 Fragility curves based on lateral strength capacity for the whole sample

near collapse point for the acceleration-displacement EC8 response spectrum with ductility $\mu = 2$. These are depicted in Fig. 20 for each building with reference to the structure type. It can be seen that while most of the UFB and DS4 representative *NC* points are to the right of the target performance point, for rubble buildings these mostly lie on the left, predicting collapse. As the number of collapses observed is definitely smaller than that computed the data is further analysed to quantify the error, as shown in Table 3.

The statistical difference between observation and prediction of the damage scenario can be explained by means of the variability of the strong ground motion within the city centre, and hence with the uncertainty implicit in using only one record. However uncertainties are also associated to the process of observing and estimating damage. In the first case damage can be underestimated because the street survey cannot take into account damage which occurred within the building, such as detachment of vertical structures from floors and from internal load bearing partitions, as this is not readily visible from the street. This, if accounted for, would likely shift the level of damage from D2 to D3 in some cases. Moreover for the small portion of the sample assessed by photographic documentation, again damage can be overlooked or underestimated, depending on the quality and orientation of the photo, especially for the lower damage grades. On the other hand the estimate of the damage state as defined is very sensitive to relatively small variation of the ductility value. For instance, an increase in ductility of 15% from 2 to 2.3 for all structure types would lead to an increase of the estimate of correct state of damage to 36% from 25%, while the overestimates would reduce to less than 50% overall.

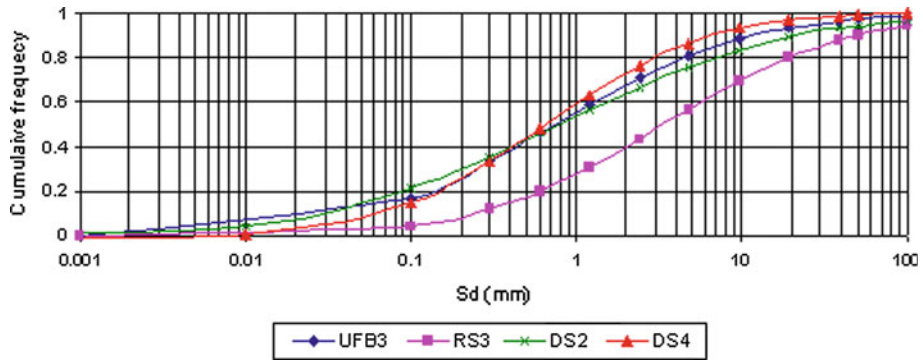


Fig. 22 Fragility curves based on displacement at damage limitation

3.4 Fragility curves

The assessment of structural vulnerability of classes of buildings is particularly useful if fragility curves can be derived which are useful to predict such classes' behaviour in different shaking scenarios. However when analysing the damage data of one specific event, only one point of one fragility curve for a given structure type can be obtained. For this reason fragility curves are derived either empirically, using statistical analysis of observed damage, or analytically by randomly generating parameters' values to feed to a given model. In the present study fragility curves are derived both in terms of lateral capacity and displacement on the basis of the distribution of performance points of each capacity curve for each wall of the given sample (Fig. 22). For lateral capacity, curves are produced for the whole sample using the average capacity curve performance points and the cumulative standard deviation. Typically fragility curves for lateral capacity are derived either in terms of PGA or in terms of Pseudo Spectral Acceleration (PSa). The latter has physical meaning if undamped linear systems are considered, as it is defined as the product of the maximum spectral displacement times the natural frequency of the SDOF oscillator. In the current application the average value of the natural frequency within the sample is used for each damage state.

For damage limitation DL, the calculated A_y , i.e. the lateral capacity at the elastic limit is used. For structural damage SD, the value of A_u corresponding to this performance point for each element in the sample is used, and for NC, near collapse performance, the peak value of the smoothed capacity curves are used. However the definition of the collapse fragility curve is more complex, because, as stated in Sect. 3.2, on the basis of the modelling assumed, there is no clear definition of the path from near-collapse capacity to collapse. Hence the collapse fragility curve is derived from the near-collapse fragility curve by assuming its central value is equal to the central value of the near-collapse curve plus 1 standard deviation of the near-collapse distribution, i.e.

$$D_c = D_{nc} + \delta_{nc} \quad 3$$

and same standard deviation, so that the cumulative fragility curve can then be derived as

$$F(D_c) = \sum_{i=1}^n \frac{1}{\delta_c} \ln \left(\frac{D_c}{S_a} \right) \quad 4$$

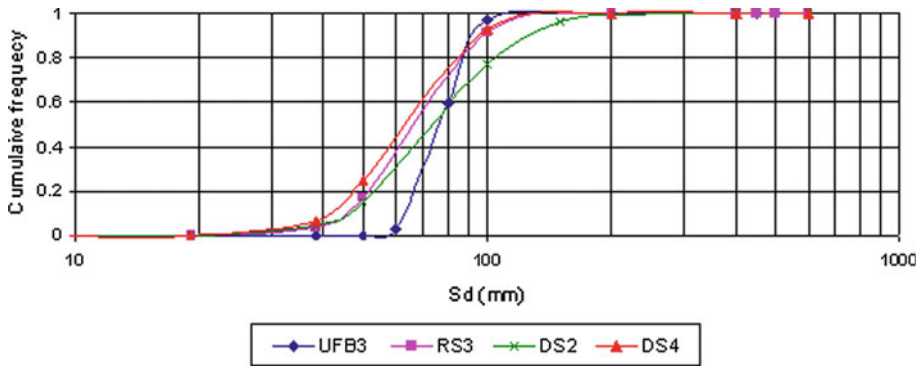


Fig. 23 Fragility curves based on displacement at structural damage

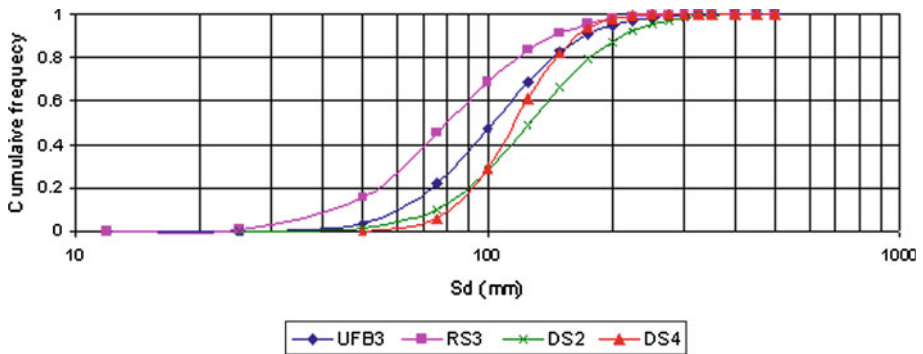


Fig. 24 Fragility curves based on displacement at collapse

where $F(D_c)$ is the cumulative distribution for collapse, D_c is the acceleration triggering collapse damage state, $\delta_c = \delta_{nc}$ is the standard deviation of the collapse distribution, S_a is the spectral amplitude, the sum is calculated over the sample. Curves are shown in Fig. 21. It can be seen that the central value for the SD curve (i.e. 50% of the cumulative distribution), is reached for a value of 0.20 g, while state C would be reached for 0.35 g. Comparing this values with the observed damage further highlights the importance of considering ductility and non linear spectra and of deriving fragility curves in terms of displacement.

In order to calculate the fragility functions in terms of displacement, D_y is used to calculate the fragility functions corresponding to damage limitation DL, Δ_u is used for significant damage SD and Δ_c is used for collapse. The curves obtained are shown in Figs. 22, 23, 24 for each structure type.

It can be seen that the greater standard deviation and ductility of the structure type DS2 clearly results in a less steep fragility curve especially at collapse. The poor performance of rubble masonry is also clearly highlighted at collapse. However for the limit state of structural damage the difference between RS3, DS4 and UFB3, is modest.

4 Discussion and conclusions

A limit state analysis of a sample of buildings in the historic city centre of L’Aquila has been conducted with the aim of assessing their seismic capacity and defining their damage patterns.

Such type of analyses is useful to ascertain the weaknesses and vulnerabilities of different buildings, following an earthquake to help defining repair and strengthening strategies. The definition of capacity curves and performance points allows an assessment of the historic building stock using the same methodology and parameters as for modern engineered structures. In particular the derivation of fragility curves both in terms of lateral strength capacity and lateral displacement is useful to extend the results to the rest of the building stock and to quantify and prioritise intervention in relation to expected seismic risk. The FaMIVE procedure shows good agreement in terms of both predicted levels of vulnerability and predicted collapse mechanisms, indicating that the correct simulation of connections and boundary constraints for the facades is a necessary but also sufficient condition to predict their failure behaviour with a limit state analysis. This allows inexpensive numerical assessments to be conducted on relatively large numbers of buildings, even though the values of their mechanical parameters are not known with any certainty. The evaluation of the correct collapse state is highly sensitive to the level of ductility assumed. The use of values typically recommended in codes of practice leads to overestimates of damage.

Acknowledgments The Authors wish to thank the Comune di L'Aquila, the Protezione Civile, the Fire Brigade Services, the University of Padova Prof. Modena's team, for providing access and logistical support during the on site survey campaigns. Thanks go to Ing. Domenico Visioni, Ing Marco Casaldi and Dr. Elena Speranza, who have provided some important insight in typical construction details used in L'Aquila and other background information, finally Ing. Viviana Novelli is thankfully acknowledged for support with the graphical output.

Appendix

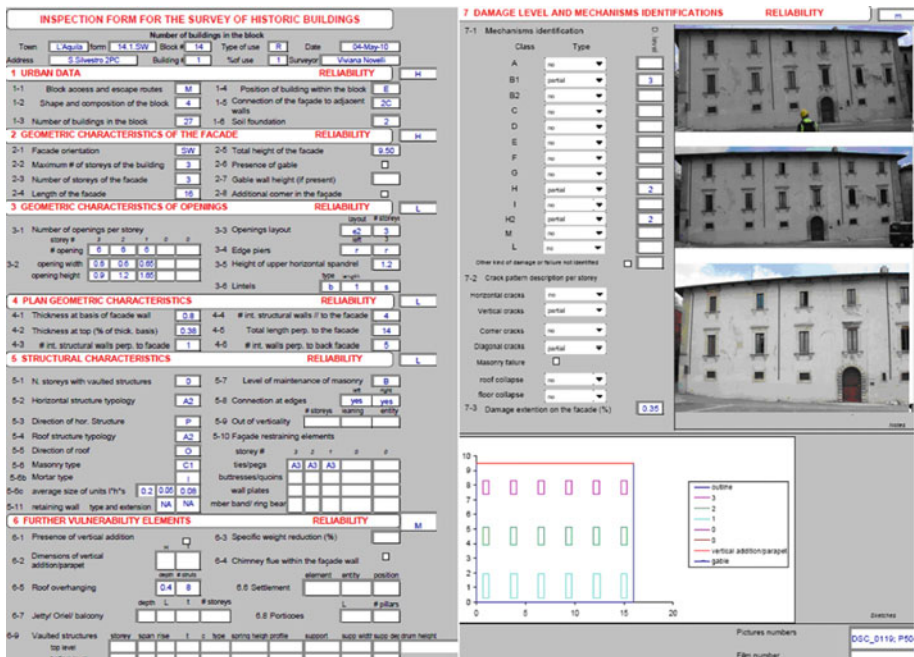


Fig. 25 Survey form used to collect the data for the FaMIVE analysis

References

- Baggio C, Bernardini A, Colozza R, Corazza L, Della Bella M, Di Pasquale G, Dolce M, Goretti A, Martinelli A, Orsini G, Papa F, Zuccaro G (2000) Manuale di istruzioni per la compilazione della scheda di 1° livello di rilevamento del danno, pronto intervento ed agibilità nell'emergenza post-sismica (AeDES). Dipartimento della Protezione Civile
- Bernardini A (ed) (2000) La vulnerabilità degli edifici: valutazione a scala nazionale della vulnerabilità sismica degli edifici ordinari. CNR-Gruppo Nazionale per la Difesa dai Terremoti, Rome
- Bernardini A, Lagomarsino S (2008) The seismic vulnerability of architectural heritage. *Proc Inst Civil Eng Struct Build* 161(SB4):171–181
- Binda L, Modena C, Casarin E, Lorenzoni F, Cantini L, Munda S (2010) Emergency actions and investigations on cultural heritage after the L'Aquila earthquake: the case of the Spanish Fortress. *Bull Earthquake Eng*. doi:10.1007/s10518-010-9217-3
- Casapulla C, D'Ayala DF (2006) In-plane collapse behaviour of masonry walls with frictional resistance and openings. In: *Structural analysis of historical construction V*, Nov 2006, Delhi. MacMillan, India
- Crowley H, Pinho R, Bommer JJ (2004) A probabilistic displacement-based vulnerability assessment procedure for earthquake loss estimation. *Bull Earthq Eng* 2(2):173–219
- D'Ayala D (2008) Seismic Vulnerability and Risk Assessment of Cultural Heritage Buildings in Istanbul, Turkey. In: *Proceedings of the 14th world conference on earthquake engineering*, Beijing October 2008
- D'Ayala D (2005) Force and displacement based vulnerability assessment for traditional buildings. *Bull Earthq Eng* 3(3):235–265
- D'Ayala D, Kansal A (2004) Analysis of the seismic Vulnerability of the architectural Heritage in Buhj, Gujarat, India, IV. *Structural analysis of historical construction conference proceedings*, pp 1069–1078
- D'Ayala D, Spence R, Oliveira C, Pomonis A (1997) Earthquake loss estimation for Europe's historic town centres. *Earthq Spectra* 13(4):773–793
- D'Ayala D, Speranza E (2003) Definition of collapse mechanisms and seismic vulnerability of historic masonry buildings. *Earthq Spectra* 19(3):479–509
- D'Ayala D, Speranza E (2002) An integrated procedure for the assessment of seismic vulnerability of historic buildings. In: *Proceedings of 12th European conference of earthquake engineering*, Paper Reference 561. Elsevier Science Limited, London
- D'Ayala D, Ansal A (2009) Non linear push over assessment of historic buildings in Istanbul to define vulnerability functions, in earthquake and tsunami, international conference, Istanbul Turkey 2009
- D'Ayala DF, Yeomans D (2004) Assessing the seismic vulnerability of late Ottoman buildings in Istanbul, IV. In: *Structural Analysis of Historical Construction Conference Proceedings*, pp 1111–1119
- Dolsek M, Fajfar P (2004) Simplified non-linear seismic analysis of infilled reinforced concrete frames. *Earthq Eng Struct Dyn* 34(1):49–66
- ENV (2005) Eurocode 8: Design of structures for earthquake resistance—Part 1-1: General rules—Seismic actions and general requirements for structures. ENV 1998-1, CEN: Brussels
- Grunthal G (1998) European Macroseismic Scale 1998. In: *Cahiers du Centre Europ. de Géodyn. et de Séismologie*, vol 15
- Lagomarsino S, Giovinazzi S (2006) Macroseismic and mechanical models for the vulnerability and damage assessment of current buildings. *Bull Earthq Eng* 4(4):415–443
- Lang K, Bachmann H (2004) On the seismic vulnerability of existing buildings: a case study of the City of Basel. *Earthq Spectra* 20(1):43–66
- Magenes G (2006) Masonry building design in seismic areas: recent experiences and prospects from a European standpoint. Keynote 9, First European Conference on Earthquake Engineering and Seismology, Geneva, Switzerland, 3–8 September 2006
- Ministry for Cultural Heritage and Activities (2007) Guidelines for evaluation and mitigation of seismic risk to cultural heritage. Gangemi Editor, Rome
- OPCM (2003) No. 3274, March 20, 2003. Official Bulletin no. 105, May 10, 2003 (in Italian)
- OPCM (2005) No. 3431, May 3, 2005. Official Bulletin no. 107, May 10, 2005 (in Italian). *Gazzetta Ufficiale—Serie Generale n. 105 (Suppl. Ordinario n. 72)*
- Pagnini L, Vicente R, Lagomarsino S, Varum H (2008) A mechanical method for the vulnerability assessment of masonry buildings. In: *Proceedings of 14th world conference on earthquake engineering*, Beijing, China
- Protezione Civile (2006) Scheda per il rilievo del danno ai beni culturali—Palazzi, Mod. B-DP, accessed on <http://www.protezionecivile.it/cms/attach/bdp.pdf> (viewed 18/03/2010)
- Restrepo-Vélez LF (2003) A simplified mechanics-based procedure for the seismic risk assessment of unreinforced masonry buildings. PhD dissertation. ROSE School, University of Pavia, Italy
- Spence R, Brun B (2006) The RISK-UE project, Special Issue. *Bull Earthquake Eng* (2006) 4:319–463

- Spence R (ed) (2007) Earthquake disaster scenario predictions and loss modelling for urban areas. LessLoss Report 2007/07, July 2007, IUSS Press
- Spence R, So E, Cultrera G, Ansal A, Pitilakis K, Costa AC, Tonuk G, Argyroudis S, Kakderi K, Sousa ML (2008) Earthquake loss estimation and mitigation in Europe: a review and comparison of alternative approaches. In: 14th world conference on earthquake engineering: innovation practice safety
- Stucchi et al (2007) DBMI04, il database delle osservazioni macrosismiche dei terremoti italiani utilizzate per la compilazione del catalogo parametrico CPTI04. <http://emidius.mi.ingv.it/DBMI04/>. Quaderni di Geofisica, 49, pp.38
- Tertulliani A, Arcoraci L, Berardi M, Bernardini F, Camassi R, Castellano C, Del Mese S, Ercolani E, Graziani L, Leschiutta I, Rossi A, Vecchi M (2010) An Application of EMS98 in a medium-sized city: the case of L'Aquila (Central Italy) after the April 6, 2009 Mw 6.3 earthquake. Bull Earthquake Eng. doi:[10.1007/s10518-010-9188-4](https://doi.org/10.1007/s10518-010-9188-4)
- Tomažević M, Bosiljkov V, Weiss P (2004) Structural Behaviour Factor for Masonry Structures. In: 13th World conference on earthquake engineering, Vancouver, Canada, paper no. 2642